JAAS

Journal of Analytical Atomic Spectrometry

Accepted Manuscript

This article can be cited before page numbers have been issued, to do this please use: I. Abad-Álvaro, D. Leite, D. Bartczak, S. Cuello, B. Gomez-Gomez, Y. Madrid, M. Aramendía, M. Resano and H. GOENAGA INFANTE, *J. Anal. At. Spectrom.*, 2021, DOI: 10.1039/D1JA00068C.

An insight into the determination of size and number concentration of silver nanoparticles in blood using single particle ICP-MS (spICP-MS): Feasibility of application to samples relevant to *in vivo* toxicology studies

I. Abad-Alvaro*[1], D. Leite[2], D. Bartczak[1], S. Cuello-Nunez[1], B.Gomez-Gomez[3], Y. Madrid[3], M. Aramendia[2,4], M.Resano[2] and H. Goenaga-Infante*[1]

1 LGC, Queens Road, Teddington; Middlesex, TW11 0LY, United Kingdom. E-mail: Isabel.AbadAlvaro@LGCGroup.com; Heidi.Goenaga-Infante@LGCGroup.com

2 University of Zaragoza, Aragón Institute of Engineering Research (I3A), Department of Analytical Chemistry, Pedro Cerbuna 12, 50009 Zaragoza, Spain.

3 Department of Analytical Chemistry, Faculty of Chemistry, Complutense University of Madrid (UCM), Av. Complutense s/n, 28040, Madrid, Spain.

4 Centro Universitario de la Defensa de Zaragoza, Academia General Militar de Zaragoza, Carretera de Huesca s/n, 50090 Zaragoza, Spain.

ABSTRACT

Toxicological studies concerning nanomaterials in complex biological matrices usually require a carefully designed workflow that involves handling, transportation and preparation of a large number of samples without affecting the nanoparticle (NP) characteristics, as well as measurement methods that enable their reliable characterisation. This work describes method development for the determination of number concentration and size of silver nanoparticles (AgNP) in blood for the purpose of application to the typical workflow of an *in vivo* toxicology assessment involving blood-containing AgNP and Ag(I) leached out from medical devices. A systematic comparison of single particle detection using millisecond *versus* microsecond dwell times in the presence of different ionic Ag [Ag(I)]-to-AgNP ratios by spICP-MS was undertaken to achieve sufficient selectivity for the determination of NP number concentration. This was achieved for the first time in a complex media such as 2.5% tetramethylammonium hydroxide (TMAH)/0.1% Triton X-100 (*v/v*) diluent, which was proven to preserve nanoparticle stability upon 8 days of storage following AgNP quantitative extraction from the blood matrix. The potential of microsecond dwell time for improved discrimination of AgNP (40 nm) from Ag(I) was demonstrated for ionic to nanoparticle ratios [Ag(I)/AgNP] of up to 106-fold. For NP sizing, a systematic study of the impact of matrix-matched ionic calibration on the derived particle size by spICP-MS is also described. Three different ionic calibration media including 1% HNO_3 (*v/v*), 1 mM trisodium citrate and 2.5% TMAH/0.1% Triton X-100 (*v/v*) were tested. Student t-test evidenced statistically significant differences between the slope of the calibration curve of Ag(I) in TMAH/Triton X-100 compared to HNO_3 and trisodium citrate matrices, whereas no significant differences were found between the two latter media. Moreover, a good agreement was found between the particle diameter derived from spICP-MS

following ionic calibration in TMAH/Triton X-100 and the diameter obtained with transmission electron microscopy (TEM), demonstrating the importance of matrix-matched calibration for NP size determination in a complex matrix using spICP-MS. Number concentration recovery measurements on blood samples spiked with AgNP and size measurements both using spICP-MS demonstrated the feasibility of the methodology developed here for potential future application to AgNP characterisation in toxicology research.

INTRODUCTION

Continuous improvements from scientific, commercial and industrial perspectives have turned nanotechnology into an important and attractive tool for overcoming social, environmental, health and economic challenges. Due to their high surface area and their nanoscale size, NP show unique physical and chemical properties if compared to bulk forms of the same material. For this reason, engineered nanomaterials (ENM) have found an important role in different industrial fields and new range of technologies, being employed from catalyst and electronic, to food, medical and cosmetic applications.[1-3] Despite the wide variety of use of ENM, there is still a lack of information regarding fate, toxicity and the consequent possible risk of these materials on environment and human health.[4-6] The widespread use of these NM has led to safety concerns with regards to their unintentional and uncontrolled release from the commercial product and potential impact on human and the environment, deserving special attention from regulatory agencies such as the European Commission and the U.S. Food and Drugs Administration (FDA).[7-9]

Due to their well-known antibacterial and antimicrobial properties, silver-based ENM are widely used in variety of products, mainly related to medical, hygiene and food.[10,11] Blood silver levels ranging from 0.1 to 23 μg L^{-1} have been reported in literature for occupationally exposed to silver workers (*e.g.* silver reclamation, jewellery manufacture, bullion production, silver chemical manufacture, production of tableware industries).[12] Its biocidal activity has made silver nanoparticles (AgNP) one of the most used type of ENM worldwide. Among them, polyethylene glycol (PEG)-coated AgNP have often been utilised for biomedical applications, since PEGylation can significantly improve NP circulation lifetime, resulting in a better systemic delivery.[13,14] Introduction of AgNP into medical devices over the recent years has raised health concerns due to the likelihood of NP release into the blood stream and/or accumulation in tissues. On the other hand, toxicity of AgNP to living organisms still remains an unsolved question, due to the fact that AgNP suspensions eventually become mixtures of Ag(I) ions, particles, aggregates plus an insoluble fraction (*e.g.* chloride salt), which makes it difficult to determine what type of toxicity is related to the nano-form and what is associated with the ions.[15,16] Therefore, there is an urgent need to develop analytical methodologies enabling quantitative assessments of release and exposure to AgNP/Ag(I). For this purpose, reliable extraction methods that ensure isolation of

particles from the components of the biological matrix sample, without changing the particle characteristics and maintaining their integrity are required.[17] The use of alkali and/or enzymatic solubilisation is often reported in the literature for releasing NP from biological matrices. Tetramethylammonium hydroxide (TMAH) is the most reported media for alkali extraction,[18-21] whereas the use of proteases, such as proteinase K, collagenase and/or hyaluronidase are the most attractive choices for enzymatic extractions.[20,22,23] However, the use of enzymes is rather expensive and therefore, alkaline extraction is often preferred when a large number of samples (*e.g.,* those from a toxicology study) need to be processed and analysed within their often short stability window.

Although the number of techniques available for nanoparticle characterisation is vast, their limitations become evident when facing the analysis of ENM in real biological samples.[24] Aspects related to time of analysis, costs (of analysis, instrumentation and maintenance), limits of detection, elemental specificity and compatibility with complex matrices still need further consideration.[25] For this reason, single-particle inductively coupled plasma mass spectrometry (spICP-MS) has emerged as a powerful tool for particle characterisation in the past decade.[26-28] SpICP-MS offers elemental specificity, high sensitivity for detecting particles at low concentrations often seen in the *in vivo* samples, particle-by-particle measurements, simultaneous information on particle number-concentration, mass concentration, and mass of individual particles correlated with spherical size equivalent, as well as number-based size distributions. Moreover, spICP-MS is one of very few techniques capable to differentiate particles and the dissolved species of the element within the same run, provided that good detection selectivity is achieved. This is particularly important in toxicological assessment and, in gaining deeper knowledge of the fate and behaviour of ENM. Although systematic comparisons, studying the impact of the instrument dwell time on the selective analysis of nanoparticle populations in suspensions containing increased amounts of dissolved analyte with spICP-MS can be found in the literature,[29,32] most studies have been conducted with particles suspended in water or other simple media. To date little is known about the capability of spICP-MS to selectively detect nanoparticles in complex matrices (*e.g.*, complex alkaline extracts) as often required for *in vivo* studies involving low nanoparticle concentrations and nanoparticles that easily dissolve and/or are associated with important blank contributions (*e.g.*, Ag, Si, Zn NP).

Following selective detection of the nanoparticle population with spICP-MS, their number-based concentration and equivalent spherical diameter (if additional information about their composition and density is known) can be determined following one of several available calibration approaches.[33-35] The most common ones for calculating size involve the use of (i) particle standards of different sizes to generate a calibration curve of signal intensity versus particle diameter, or (ii) elemental standard solutions containing analyte in the dissolved form. The latter approach has been found easier to implement and therefore, often used since commercially available well-characterised particle Reference Materials (RM) are scarce.[36] However, the impact of potential matrix effects on the accuracy of particle mass and, corresponding size in the presence

of complex matrices (*e.g.,* with high slurry content, high concentration of organic materials and solvents or strongly acid/alkaline solutions) needs further investigation.[34,38,39]

Different strategies for overcoming matrix effects in ICP-MS have been reported in the literature, including sample pre-treatment (*e.g.*, precipitation, dilution, liquid-liquid extraction (LLE), solid-phase extraction (SPE), cloud-point extraction (CPE)), use of different sample introduction systems, instrument optimisation and/or the use of different calibration strategies by internal standardisation, standard addition, isotope dilution and matrix-matched calibration.[40] Out of all the approaches reported so far, matrix-matching is the easiest and the most cost- and time-effective to implement for the purpose of higher throughput routine analysis, whenever it is feasible (*e.g.*, the matrix composition is known in advance and it is easy to duplicate).[41] However, to date, there are very few literature reports relevant to toxicological studies that investigate the application of matrix-matched calibration to particle size determination using spICP-MS reporting different findings. Vidmar *et al.*[20] investigated the characterisation of AgNP in human tissue by spICP-MS after enzymatic and alkaline digestion. Transport efficiency using AuNP in ultrapure water, 1.0% TMAH (*v/v*) and enzyme solution, as well as the corresponding dissolved Ag and Au standards in these media were considered. An important increase in the response for ionic Au in 1% TMAH (*v/v*) was observed, suggesting a stabilising effect for the Au ions and a reduction of losses of Au ions in the sample introduction system. However, this effect was not observed for NP. On the other hand, a decrease in sensitivity for ionic Ag in the 1% TMAH (*v/v*) medium compared to water was reported likely due to adhesion of silver ions to the sample introduction system, but the same behaviour was not observed for the NP. In the absence of behaviour correlation between the dissolved and nanoparticulate samples in presence of the complex diluent/matrix, particle size values were calculated without matrix-matched calibration. Liu *et.al.*[38] investigated matrix effects on AgNP and Ag(I) intensities with diluents that simulate biological and environmental media, such as water, 1 mM tris(hydroxymethyl)aminomethane, borate buffer, sodium carbonate buffers solutions, 1 mM sodium citrate, 1 mM sodium chloride, 1 mM glutathione and 0.1 mM sodium sulphide. The matrix-matched approach was not suggested in this study as verified losses in the ionic intensity due to the interaction of Ag(I) with matrix compounds occurred, whereas the NP intensity remained the same for all the tested media. On the other hand, Montaño *et. al.*[34] reported that if calibration solutions are not matched to the sample matrix this may result in an error in the measured NP size and pointed out that the matrix-matched effects on the accuracy of NP size need further assessment. In this line, Loula *et. al.*[45] recommended the use of calibration solutions with similar matrix to that of the NP in order to overcome the effect of non-spectral interferences.

This work describes systematic method development for the determination of both nanoparticle number concentration and size, for the purpose of application to an *in vivo* toxicology study involving blood-containing AgNP and Ag(I) leached out from medical devices. To achieve this, AgNP of different sizes (40 nm and 75 nm) in blood extracts containing 2.5% TMAH/0.1% Triton

View Article Online
DOI: 10.1039/D1JA00068C

X-100 were selected as target samples. This medium is studied here for the first time as it has been proven to enable efficient extraction of AgNP from blood and preserve nanoparticle stability up to 8 days of extract storage during previously unreported studies in the author's laboratory. The impact of using millisecond *versus* microsecond instrument dwell times on the quality of NP number concentration data in the presence of different Ag(I)-to-AgNP ratios in the complex 2.5% TMAH/0.1% Triton X-100 diluent by spICP-MS is investigated here for the first time. Moreover, in order to obtain reliable particle size (derived from mass) information, a systematic study of the impact of matrix-matched ionic calibration is presented, using the same alkaline medium, in comparison with 1% HNO_3 (*v/v*) and 1 mM trisodium citrate. The feasibility of the methodology developed was investigated for the workflow required for AgNP characterisation in blood from an *in vivo* toxicology study. To achieve this, recovery of particle number concentration and size were measured for two scenarios involving spiking of Seronorm™ human-matrix blood with PEG-AgNP (40 nm) at concentrations relevant to those of *in vivo* toxicology assessment and *i)* storage at 4 °C during 8 days followed up by NP extraction and analysis using spICP-MS or, *ii)* NP extraction followed up by storage of extracts at 4 °C during 8 days before analysis by spICP-MS. Results were compared with those obtained for extraction and analysis performed on freshly spiked samples. Nanoparticle recovery experiments on rat blood samples from a toxicological study were also undertaken.

EXPERIMENTAL

Reagents and materials

AgNP with a nominal diameter of 75 nm was obtained from NIST (NIST, Gaithersburg, USA - RM 8017 polyvinylpyrrolidone coated). Certificate of analysis provided by NIST reports a size of 74.6 ± 3.8 nm measured by transmission electron microscopy (TEM). Suspensions of monodisperse PEG coated, NanoXact™, AgNP of nominal diameter 41 ± 4 nm (TEM value provided by the manufacturer on the Certificate of Analysis) were purchased from nanoComposix (nanoComposix, San Diego, USA).

Ultrapure water (18 MΩ, 25 ^{0}C) was obtained from an Elga water purification unit (Elga, Marlow, Buckinghamshire, UK). A 25% *v/v* aqueous solution of electronic grade TMAH was obtained from Alfa Aesar GmbH & Co KG (Lancashire, UK), whilst Triton X-100 was purchased from Sigma-Aldrich (Sigma-Aldrich, Gillingham, UK). Suprapure grade HNO_3 was purchased from Romil (Romil Ltd., Cambridge, UK) and sodium citrate tribasic dihydrate with purity higher than 99.5% *w/w* from Sigma-Aldrich (Sigma-Aldrich, Gillingham, UK) was also used. Ionic solutions were prepared from a standard stock solution of 984.5 µg g^{-1} (Romil Ltd., Cambridge, UK). Seronorm™ Trace Elements in whole blood, level 2 was purchased from Sero AS (Sero AS, Billingstad, Norway, lot 1406264) and used as a model blood sample.

View Article Online
DOI: 10.1039/D1JA00068C

Instrumentation

An Agilent 8900 ICP-MS/MS (Agilent Technologies, Tokyo, Japan) was used throughout. The sample introduction system consisted of a MicroMist nebuliser and cooled (2 °C) spray chamber. The instrument was tuned daily for optimum signal intensity and stability. Instrument operating parameters are listed in Table 1. Analyses were performed using dwell times of 3 ms and 100 µs, with no settling time between measurements. Total acquisition time was fixed at 60 s. Isotope ^{107}Ag in no gas mode was monitored. Single Particle Application Module for ICP-MS MassHunter 4.3 (version:G72Dc.c.01.03) software, as well as *in-house* developed Excel 2016 (Microsoft, Redmond, USA) spreadsheets were used for data processing. OriginPro 2020 data analysis software (OriginLab Corporation, Northampton, USA) was also used.

Transport efficiency was calculated according to the particle frequency method developed by Pace *et al.*[33] against NIST RM 8017 in 2.5% TMAH/1% Triton X-100 (*v/v*). Dynamic mass flow method (DMF), which uses no reference material for the calculation of transport efficiency, was used for the *in-house* characterisation on particle number concentration of this material,[42] obtaining a particle number concentration of (4.31 ± 0.34) x 10^{14} kg^{-1} (mean ± standard measurement uncertainty 'u'; k=1) which was in a good agreement with the value indirectly calculated from NIST data. The sample mass flow rate was daily calculated by weighing the mass of diluent (TMAH/Triton) taken up by the peristaltic pump for two minutes. This operation was performed in triplicate and the average value used in calculations. Under the experimental conditions used in this work, the transport efficiency was (11.7 ± 0.5)% at a sample flow rate of 0.35 g min^{-1}.

Procedures

Sample dilution. NIST RM 8017 suspension was reconstituted by addition of 2 mL ultrapure water followed by hand shaking for 60 s, as indicated in the material certificate. It was let stand for one hour prior use and then stored at 4 °C in the dark. Vials containing AgNP suspensions were gently inverted several times to ensure homogeneity of the suspension. Prior to analysis, suspensions were gravimetrically diluted using an analytical balance (4-decimal places). Following the approach recommended by Abad-Alvaro *et al.*[29] and considering linear range previously studied for this instrument,[42] the optimal dilution factor for 75 nm NIST RM 8017 and 40 nm PEG AgNP (1.8 x 10^7 and 1.7 x 10^6, respectively) were selected to achieve an optimal NP flux, so that the impact of formation of NP double and triple events was minimal. The final concentrations of NP in the working solutions (after dilution) were around 2.4 x 10^7 kg^{-1} and 3.5 x 10^7 kg^{-1} for NIST RM 8017 and 40 nm PEG AgNP, respectively. Diluted suspensions of AgNP were prepared in 2.5% TMAH/0.1% Triton X-100 (*v/v*). Ionic silver calibration curves ranging from 0 to 10 µg kg^{-1} were performed in 1 mM citrate, 1% HNO_3 (*v/v*) and 2.5% TMAH/0.1% Triton X-100 (*v/v*) on three different days. Statistical comparison between sensitivities among different media was performed by looking at

View Article Online
DOI: 10.1039/D1JA00068C

variability in the slopes of the calibration curves from three different days following student t-test (at 95% confidence level).

Preparation of AgNP/Ag(I) mixtures. For the preparation of suspensions at different Ag(I)-to-AgNP ratios in 2.5% TMAH/0.1% Triton X-100 (*v/v*), particle number concentration was kept constant (2.4 x 10^7 kg^{-1} and 3.5 x 10^7 kg^{-1} for NIST RM 8017 and 40 nm PEG AgNP, respectively), while increasing the amount of dissolved Ag. Ionic Ag(I) concentrations ranged from 0.5 to 9 µg kg^{-1} for suspensions containing the NIST RM 8017 (75 nm) and from 0.5 to 2.8 µg kg^{-1} for suspensions containing 40 nm PEG AgNP. All these additions were performed with ionic Ag(I) prepared in the same TMAH/Triton medium as the NP. Larger additions of Ag(I) were also considered and studied, but they are not discussed in this work as no selective detection of NP was achieved due to high signal intensity of dissolved Ag. Suspensions were immediately analysed upon dilution.

Extraction of AgNP from blood. All blood samples were prepared in a class II cabinet. The content of vials containing of Seronorm™ blood was suspended in 3 mL of ultrapure water, according to manufacturer's instructions. Approximately 0.1 g of blood were spiked with 40 nm PEG AgNP (*in-house* characterised on particle number concentration by the dynamic mass flow method, which uses no reference material for the calculation of transport efficiency[42]) to aid final AgNP concentration of 10 µg kg^{-1} or 0.1 µg kg^{-1}. Blood samples were digested by mixing with 0.6 mL of 15-25% TMAH (*v/v*) per 0.1 g of blood followed by 5 min sonication in an ultrasonic bath and 24 h incubation at room temperature in the dark. Following digestion in TMAH blood samples were diluted to a final weight of 6 g with 0.1% Triton X-100 (*v/v*). Samples spiked with 0.1 µg kg^{-1} PEG-coated AgNP were analysed without any further dilution, whilst samples spiked with 10 µg kg^{-1} were diluted with 2.5% TMAH/0.1% Triton X-100 (*v/v*) prior to analysis. To assess the impact of storage on sample stability, blood digests were stored for up to 8 days at 4 °C in the dark prior to analysis, and/or spiked blood samples were stored for 8 days at 4 °C in the dark prior to digestion and analysis. Three separate sample preparations were analysed.

To verify the validity of the method for real blood samples, control rat blood samples from a toxicological study were also digested following the procedure described above. Approximately 3 g of digested control blood were spiked with 1.5 µg kg^{-1} Ag(I) and 4.5 x 10^7 kg^{-1} PEG-coated AgNP.

RESULTS AND DISCUSSION

Selection of the NP extraction media

When working with ENM, one of the main aspects to consider is their behaviour and stability in different media. NP can suffer from transformations (*e.g.*, dissolution, agglomeration, aggregation,

surface modification, complexation) along their life cycle and depending on the dispersant medium.[24] Facing samples containing NP from a toxicological study, such as ENM/ionic mixtures in animal blood, these changes can occur during storage and particle extraction. During extraction, alkaline reagents, such as TMAH, are often employed to break down organic and biological matrices, including blood. This strong base reagent causes the hydrolytic scission and methylation of ester, amide and some ether bonds and is able to break disulphide chemical bonds in proteins,[43] which makes it quite attractive for the digestion of biological samples. However, TMAH, as a strong base, could produce the precipitation of silver. For this reason, it usually needs the presence of a surfactant in order to maintain the integrity of the AgNP. The effect of the extraction/digestion media containing TMAH and Triton-X 100 surfactant on AgNP stability was studied. Based on the literature[17] and on previous experience in the author's laboratory 1% TMAH/0.1% Triton X-100 (*v/v*) and 2.5% TMAH/0.1% Triton X-100 (*v/v*) were selected, respectively, for further investigation in comparison with water and only 0.1% Triton X-100. The latter has been proven useful to keep AgNP stable when extracted from animal samples of low AgNP content where further media dilution is not possible (unreported data). Higher amounts of TMAH were not considered for their introduction in the ICP-MS due to the corrosive nature of this reagent.

Figure 1 shows signal distribution histograms corresponding to NIST RM 75 nm AgNP suspensions (particle number concentration of 2.5 x 10^7 NP kg^{-1}) in ultrapure water, 0.1% Triton X-100 (*v/v*), 1% TMAH/0.1% Triton X-100 (*v/v*), and 2.5% TMAH/0.1% Triton X-100 (*v/v*). The occurrence of multiple events was avoided working with sufficiently diluted suspensions. As observed in this figure, AgNP distributions in TMAH/Triton X-100 (Fig. 1 c-d) are shifted to the right, towards higher particle signal intensity. This is due to an enhancement of the Ag sensitivity, which was observed for both AgNP and ionic Ag to the same extent when the TMAH/Triton X-100 was present. This fact also supports the need of using matrix matching of ionic calibration for particle size determination, which will be further discussed in the manuscript. On the other hand, the signal distribution histograms show a secondary population next to the main particle fraction (see Fig. 1 a-b) when TMAH is not present in the medium. This suggests destabilisation of the particles in ultrapure water and 0.1% Triton (*v/v*) media, resulting in formation of agglomerates/aggregates. In the case of AgNP in TMAH/Triton X-100 no evidence of agglomeration/aggregation was observed, as only one big population related to AgNP was detected. This effect is also confirmed by the number of particle events recorded (Table 2). If only the main fraction is considered, the number of particles recorded represents 81% of the total in the case of ultrapure water and 82% in the case of Triton X-100, whilst it is 100% for 2.5% TMAH/Triton and 1% TMAH/Triton. Altogether, this indicates that these two reagents, when combined, act not only as particle extractant but also as stabilising agent. Although the formation of Ag particles under alkaline conditions in the presence of alkoxides as reducing agents has been reported in the literature,[44] Vidmar *et al*.[20] demonstrated that the use of TMAH itself did not contribute to significant particle formation when Ag(I) was spiked in 1% TMAH. Likewise, Gray *et al*.[21] did not observe the formation of particles from ionic Ag when

View Article Online
DOI: 10.1039/D1JA00068C

TMAH extraction was used in beef tissue. From the two tested TMAH/Triton media, a medium containing 2.5% TMAH was chosen for further studies as it minimises the dilution factor required following sample digestion. This is particularly important when working with real samples from animal studies for which NP concentrations are relatively low.

Selective discrimination of AgNP from Ag(I) for particle number concentration determination

The feasibility of spICP-MS for the determination of particle number concentration is compromised by the achievable size limit of detection. This is critically affected by the presence of a high background signal coming from matrix-induced interferences, polyatomic interferences, procedural blanks and/or NP dissolution. The latter is well known to hamper the achievable size limit of detection of AgNP. However, working at the microsecond dwell times instead of the millisecond ones have been shown to reduce the contribution of the background signal, allowing a better discrimination between the particles and the dissolved species and thus improving the size detection limits.[29]

In order to know whether AgNP can be detected with a sufficient selectivity from Ag(I) for further determination of particle number concentration in blood digests, a systematic comparison of single AgNP detection by spICP-MS using ms and µs dwell times in the presence of different Ag(I)-to-AgNP ratios was carried out in the presence of 2.5%TMAH/0.1%Triton X-100 (*v/v*) matrix. Moreover, two different particle sizes were studied (75 nm and 40 nm) in order to demonstrate the influence of size on the selective discrimination of AgNP from ionic silver. Although systematic comparisons regarding nanoparticle suspensions with increased amounts of dissolved analyte and/or different dwell times can be found in literature,[29,32] most studies are conducted with NP in water or other simple media. However, to date little is known about the capability of spICP-MS to selectively detect nanoparticles in complex matrices (*e.g.*, complex alkaline extracts) as often required for *in vivo* studies involving low NP concentrations and NP that easily dissolve and/or are associated with important blank contributions. Figure 2 and Figure 3 show signal distribution histograms corresponding to the 75 nm (Fig. 2 a, g) and 40 nm PEG AgNP (Fig. 3 a, e) suspensions alone, and in the presence of different Ag(I) concentrations (Fig. 2 b-f, h-j; Fig.3 b-d, f-h). Time scans and signal distribution histograms of Ag(I) standards in 2.5%TMAH/0.1%Triton X-100 (*v/v*) were also obtained (data not shown) in order to discard the formation of AgNP from ionic silver solutions in this medium. The data did not suggest AgNP formation since the number of events registered over the baseline was in agreement with the ones observed for the blank (2.5% TMAH/0.1% Triton X-100). Dwell times of 3 ms and 100 µs were used throughout. According to spICP-MS theory and due to different distribution of the analyte in the aerosol droplets,[27] two different distributions should be observed in the signal distribution histograms; a first one correlated

View Article Online
DOI: 10.1039/D1JA00068C

with the background/dissolved Ag and a second one produced by the nanoparticles. The count intensity at the maximum of the first distribution increases with the concentration of the dissolved species present in the medium, as it can be observed in Figures 2 and 3. On the other hand, working at µs dwell times allows a better discrimination of AgNP from Ag(I) (Figure 2 a-f, Figure 3 a-d). Not only the dwell time, but also the NP size affects the selective detection of AgNP, being harder to differentiate the nanoparticles from the background the smaller the NP are. Table 3 includes the size limits of detection (LOD_{size}) obtained for dwell times of 100 µs and 3 ms. These were calculated for different concentrations of Ag(I) added to the NP suspensions. For these calculations, a *5σ* criterion[27,46] for spherical solid of single element was applied. The calculated LOD_{size} are supportive of the appearance of the histograms of Figure 3 f-h obtained for a dwell time of 3 ms, for which the particle distribution is partially or totally overlapped with that of Ag(I).

Table 4 and Table 5 show the number based concentration of 75 nm and 40 nm AgNP suspensions in the presence of different concentrations of dissolved species present at the part-per-billion level when measuring at a dwell time of 100 µs. A 5σ criterion was applied for discriminating between both distributions and minimise the occurrence of false positives.[45] Maximum Ag(I)-to-AgNP ratios for the selective detection of 75 nm AgNP were found at 175 [addition of 9 µg kg^{-1} Ag(I)] and 48 [addition of 2.5 µg kg^{-1} Ag(I)] (Fig. 2 e, i), when working at dwell times of 100 µs and 3 ms, respectively. For 40 nm PEG AgNP, spICP-MS was able to distinguish AgNP from Ag(I) even if the ionic silver concentration was 106-fold [addition of 1 µg kg^{-1} Ag(I)] the AgNP concentration for a dwell time of 100 µs, remaining just below 53-fold [addition of 0.6 µg kg^{-1} Ag(I)] when 3 ms were used (Fig. 3 c, e, f). In the case where the 40 nm PEG AgNP were just suspended in TMAH/Triton (Fig. 3 a, e) without addition of Ag(I), the first distribution was due not just to residual silver/blank contribution (as in the case of the 75 nm AgNP – Fig. 2 a, g), but also to the presence of Ag(I) from the dissolution of these NP in the stock suspension. Similar particle stability issues have also been reported for AgNP in bibliography.[38] The relative contribution of the dissolved fraction in 40 nm PEG AgNP was approximately 20% as determined by spICP-MS. This was taken into consideration in the calculations of the total amount of Ag(I) present in the final samples. Based on the dissolution of 40 nm PEG AgNP in the stock solution, the maximum recovery that could be achieved was of approximately 80%. Particle number concentration recoveries of over 100% were obtained when both distributions (background and nanoparticles) were not well resolved from each other, suggesting that some of the Ag(I) was accounted for as NP.

Effect of matrix matching of ionic calibration for particle size determination

SpICP-MS technique is commonly used for providing values not only related to nanoparticle number concentration, but also size. However, the technique itself measures the element mass content per particle and only if additional information is provided, such as particle composition, shape and density, the corresponding particle size can be calculated, usually as spherical

View Article Online
DOI: 10.1039/D1JA00068C

equivalent. The most commonly used approach for particle size determination is based on the calculation of two parameters: transport efficiency and the sensitivity of an ionic calibration curve. However, the effect of the ionic calibration on NP size characterisation has not been deeply studied or elucidated so far.[34] Typically, a calibration curve is produced with elemental standards diluted in ultrapure water or acid solution in order to determine the sensitivity of the analyte and relate it to NP pulse intensity and, therefore, calculate the particle mass and diameter. However, acid media are not always compatible with NP and it is not clear if a response factor determined in such simple media is the same as the one in the presence of alkali and surfactants, such as the 2.5% TMAH/0.1% Triton-X 100 (v/v) media chosen for this study. For this reason, a systematic study of the effect of matrix matching of the ionic calibration on the particle size obtained with spICP-MS was carried out. To undertake this study, three different calibration curves were prepared in three different media consisting of: 1% HNO_3 (*v/v*) (most commonly used medium for ICP-MS ionic calibration), 1 mM trisodium citrate (aqueous non-acid medium, known as both, good chelator for dissolved metal ions and as particle coating and stabilising agent) and 2.5% TMAH with 0.1% Triton X-100 (*v/v*) (used for NP extraction from biological samples and stabilisation upon storage and chosen as optimal in the study reported here, as explained in the previous paragraphs). The measurements of the three calibration curves were performed on three different days in order to detect any variability in the instrumental sensitivity and the results are shown in Figure 4.

As it can be seen in the Figure, sensitivity values obtained for ionic silver in 1 mM trisodium citrate and 1% HNO_3 (*v/v*) media were very similar, whereas that of 2.5% TMAH/1% Triton X-100 (*v/v*) was approximately 25% higher. In order to confirm any statistically significant difference among the different media, the sensitivity values of each day were normalised (all the sensitivity values were divided by the higher sensitivity value, setting the higher value as 1) and a student t-test at 95% confidence level was performed. The calculated p-values were (i) 0.8046 for HNO_3 vs citrate; (ii) 0.0461 for citrate *vs* TMAH/Triton and (iii) 0.0085 for HNO_3 vs TMAH/Triton, with $p<0.05$ considered statistically significant. This confirmed that the slope of the TMAH/Triton calibration curve was significantly different those of citrate and HNO_3 curves, whilst no statistically significant differences between the slopes of citrate and HNO_3 calibration curves were found. These results indicated that calibration performed in a typically used acid medium, would have caused in this case considerable bias in AgNP sizes prepared in the TMAH/Triton medium studied here.

From a theoretical point of view, the relationship between the signal R (ions counted per time unit) and the mass concentration C^M of a solution of an analyte nebulised into an ICP-MS can be expressed as[27]

$$R = K_{intr} K_{ICPMS} K_M C^M \quad (1)$$

where K_{intr} (= $\eta_{neb} Q_{sam}$) represents the contribution from the sample introduction system, through the nebulisation efficiency (η_{neb}) and the sample uptake rate (Q_{sam}), K_{ICPMS} is the detection

View Article Online
DOI: 10.1039/D1JA00068C

efficiency (ratio of the number of ions detected versus the number of atoms introduced into the ICP; dependent on each particular instrument), and K_M (=AN_{Av}/M_M) includes the contribution from the element measured (A, atomic abundance of the isotope considered; N_{Av} Avogrado number; M_M atomic mass). The term "K_{ICPMS} K_M" can be easily deduced from equation (1) by simply analysing dissolved analyte standards and knowing the value of K_{intr}. On the other hand, when NP suspensions are measured in time-resolved mode and one NP is detected during a single reading, the total counts per reading and NP, r_{NP}, can be expressed with respect to the mass of analyte per NP (m_{NP}) as:

$$r_{NP} = K_{ICPMS} K_M m_{NP} \quad (2)$$

or to the diameter of NP (d) if parameters such as density (ρ), mass fraction of the element in the NP (X_{NP}) and a spherical shape is assumed:

$$r_{NP} = \frac{1}{6} \pi \rho X_{NP} K_{ICPMS} K_M d^3 \quad (3)$$

According to equations 2 and 3 and considering the same value of r_{NP} for one specific NP solution in one specific medium, an increase in the term "K_{ICPMS} K_M", as found for the ionic calibration curve in the TMAH/Triton medium, would lead to lower m_{NP}, and hence, to lower sizes, whereas lower values in "K_{ICPMS} K_M" would mean higher m_{NP} and size.

The calibration curves were used to derive the size of 40 nm PEG AgNP suspended in 2.5% TMAH/1% Triton X-100 (*v/v*), acid and citrate media, as shown in Table 6. From these values, it can be seen that the diameter values only agree with the given TEM value (41 ± 4 nm) provided by the manufacturer when the ionic calibration is matrix-matched with the particles [the ionic calibration was prepared in 2.5% TMAH/1% Triton X-100 (*v/v*)]. Conversely, the calculated size values with the ionic calibration in both acid and citrate media were found to be positive biased and in disagreement (according to student t-test at 95% confidence) with the size obtained using matrix-matched calibration. These differences are better evidenced using graphical representation of the particle size distributions (Figure 5). The particle size distribution obtained in TMAH/Triton is shifted to lower particle sizes and the NP size was found to agree well with that obtained using TEM. The results presented here highlight the importance and necessity of studying the matrix-induced effects on element-sensitivity on case-by-case basis.[39] In the work reported here, higher TMAH concentration (2.5%), than those typically used in the literature (1%),[20,21] in conjunction with the effect of surfactant resulted in significant increase of the response factor measured for both Ag(I) and AgNP.

Characterisation of AgNP and Ag (I) in blood: feasibility investigation for the purpose of application to the typical workflow of an in vivo toxicology study

Toxicological studies concerning ENM in complex biological matrices usually require a carefully-designed workflow that involves handling, transportation and preparation of a large number of samples without affecting the particle characteristics. In order to overcome this challenge, a sample preparation protocol that enables digestion and/or storage of a large number of samples was developed for the purpose of application to the typical workflow of an *in vivo* toxicology study. The protocol utilised TMAH/Triton as extractant and nanoparticle stabilising agent, respectively. Particle recoveries in terms of the number-based concentration and particle stability in terms of the size and size distribution, as well as digestion and storage were investigated into spiked model blood matrix. For this purpose, blood samples spiked with different concentrations of AgNP relevant to *in vivo* toxicological studies were digested and diluted following the procedure described in the Experimental section; 2.5% TMAH/0.1% Triton-X and AgNP concentrations of 10 μg kg^{-1} or 0.1 μg kg^{-1} were used. In this case, 40 nm PEG coated AgNP were chosen because of their wide use as antibacterial agents in biomedical devices. For this study, a new batch of particles was used, so that no unintentionally added ionic silver fraction was present in the stock solution. The dynamic mass flow (DMF) method,[42] which does not require a RM for the calculation of transport efficiency, was used for the *in-house* determination of particle number concentration of this NP suspension. The number concentration of nanoparticles obtained for the 40 nm PEG AgNP standard was (5.55 ± 0.34) x 10^{13} kg^{-1} (mean ± standard measurement uncertainty 'u'; k=1) which was in a good agreement with the value reported by the supplier (5.6 x 10^{13} L^{-1}). All spICP-MS measurements were performed with a dwell time of 100 μs and matrix-matched ionic calibration, described in the previous sections.

A range of different experimental conditions were investigated when optimising the sample digestion protocol with TMAH, which involved varying its concentration and/or added quantities (data not shown). The highest recovery rates in terms of particle number concentration (over 80% when compared to the value measured with DMF method) were obtained when 15% TMAH (*v/v*) was used for the sample digestion. Table 7 shows the particle number concentration and size values obtained under optimal conditions for blood samples spiked with NP and immediately digested and analysed. Again, recoveries are calculated against the amount of the original AgNP standard suspension *in-house* characterised by DMF method. Results show that it was possible to detect and quantify the nanoparticles spiked into the blood at the levels ranging from 0.1-10 μg kg^{-1} with particle recoveries ranging from 86-98%. Although changes in the particle size distribution (Figure 6) were not detected when the blood sample was spiked with 10 μg kg^{-1} AgNP and digested, a slight decrease in the NP size was noted in the case of the sample spiked with 0.1 μg kg^{-1} AgNP.

In order to fully assess the impact of sample storage on particle stability, two different studies were carried out. At first, digested samples were stored at 4 °C in the dark for 8 days prior to analysis by spICP-MS. The summary of the obtained particle number concentration values and sizes are shown in Table 8. In the second part of the stability study, spiked blood samples were stored at 4 °C in the dark for 8 days prior to digestion with TMAH and analysis by spICP-MS (Table 9). From the results shown in Tables 8 and 9, it can be concluded that the storage of digested blood during 8 days did not affect the particle number concentration of the particles, since 88-93% of particles were recovered. However, slight decrease in sizes (Figure 7), as well as the presence of some ionic silver, were detected after these 8 days of storage. On the other hand, storage of samples for 8 days prior to digestion resulted in a significant decrease in the particle number concentration (only 12-17% was recovered), as well as decrease in size, indicating far reaching transformation of the particles in undigested blood. Overall, it can be concluded that animal blood samples from any *in vivo* toxicological study must be digested upon arrival and analysed within 8 days following digestion. This provides a stability window of several days for sample analysis which is particularly useful when the volume of samples is relatively large.

Finally, a spiking experiment with Ag(I) and AgNP was undertaken for the purpose of recovery measurements in a real blood sample. To achieve this, control rat blood sample from a toxicological study was first digested with TMAH and then diluted with Triton X-100 following the procedure described in the Experimental section. Afterwards, the digested blood was spiked with 40 nm PEG AgNP and Ag(I), in order to get a final concentration of 4.5 x 10^7 NP kg^{-1} and 1.5 µg kg^{-1}, respectively. This Ag(I) concentration was selected considering the results previously shown, where the use of µs dwell times allowed the selective discrimination of 40 nm PEG AgNP even in the presence of 1.2 µg kg^{-1} Ag(I). In this blood matrix, average recoveries of (93 ± 1)% and (110 ± 2)% were achieved for Ag(I) and AgNP, respectively (Fig. 8); confirming that spICP-MS is a powerful technique for the simultaneously determination of both particulate and ionic silver in biological samples using the methodology developed in this work. Moreover, it was demonstrated that the extraction procedure here described led to similar results in terms of NP recovery and size for different kind of blood samples (Seronorm™ human blood matrix and rat blood) spiked with AgNP.

CONCLUSIONS

Systematic method development for the determination of both nanoparticle number concentration and size has been described for the purpose of application to the typical workflow of an *in vivo* toxicology study involving blood-containing AgNP and Ag(I) leached out from medical devices. Such a workflow usually involves a large number of samples that have to be processed and analysed within their stability window.

View Article Online
DOI: 10.1039/D1JA00068C

The use of alkaline digestion of the blood samples with TMAH in combination with sample stabilisation using Triton X-100 was proven to extract the AgNP efficiently from blood as well as help preserve the particle properties in terms of size and number based concentration for up to 8 days, provided that sample digestion is performed as soon as the samples are produced. This provides a stability window of several days for sample analysis which is particularly useful when the volume of samples is relatively large.

Although the presence of dissolved species in AgNP suspensions was shown to hamper the size limits of detection, the potential of microsecond dwell time was demonstrated for the selective discrimination of small AgNP with sizes of around 40 nm in the presence of up to 106-fold excess of ionic silver (1.16 μg kg^{-1} Ag(I)/0.011 μg kg^{-1} AgNP) in the 2.5% TMAH/0.1% Triton X-100 (*v/v*) matrix. On the other hand, matrix-matched ionic calibration was found to be necessary for the reliable characterisation of AgNP in terms of size in the complex TMAH/Triton media; the sensitivity obtained for ions and NP was similarly influenced by this media so a good agreement of the spICP-MS size using matrix matched calibration agreed well with that obtained by TEM.

AUTHORS CONTRIBUTIONS

IAA, DL, DB, SCN, BGG: conceptualisation, methodology, analysis, data curation. These authors performed the experiments present in this paper; more specifically IAA and BGG undertook the study on stability of AgNP in different extraction media, as well as on the selective discrimination of AgNP from ionic silver, DL and DB carried out the experiments related to matrix-matching effects on particle sizing, whilst DB and SCN conducted the experiment related to particle stability in blood and the extraction/stabilisation protocol optimisation. IAA and DL wrote the first draft. IAA, DB, SCN, HGI contributed to writing, reviewing and editing. YM, MA: reviewing and editing. MR: reviewing, editing, resources and funding acquisition. HGI: conceptualisation, funding acquisition, project administration, methodology, resources, supervision and paper sign off for submission.

CONFLICS OF INTEREST

There are no conflicts to declare.

ACKNOWLEDGEMENTS

The work described in this manuscript was supported by UK Department for Business, Energy & Industrial Strategy (BEIS) through the Chemical and Biological Metrology Programme. The authors also acknowledge the funding from Ministerio de Economía y Competitividad (CTQ2015-64684-P (MINECO/FEDER)) and Ministerio de Ciencia e Innovación (PGC2018-093753-BI00

View Article Online
DOI: 10.1039/D1JA00068C

(MCIU/AEI//FEDER, UE)) and the Aragon Government, as well as financial support from the Community of Madrid (Spain) and European funding from FSE and FEDER programs (S2018/BAA-4393, AVANSECAL-II CM). Diego Leite acknowledges CNPq, Conselho Nacional de Desenvolvimento Científico e Tecnológico - Brazil (232487/2014-6) and Fundación Ibercaja-CAI (CB 7/18).

REFERENCES

1. P. Krystek, A. Ulrich, CC. Garcia, S. Manohar, R. Ritsema , *J Anal At Spectrom*., 2011, **26**, 1701-1721.

2. AA. Keller AA, S. McFerran, A. Lazareva, S. Suh, *J Nanoparticle Res*., 2013, **15**, 1692.

3. M. Bundschuh M, J. Filser, S. Lüderwald, MS. McKee, G. Metreli, GE. Schaumann, R. Schulz, S. Wagner, *Env Sci Eur*., 2018, **30**.

4. MJ. Gallagher, C. Allen, JT. Buchman, TA. Qiu, PL. Clement, MOP. Krause, LM. Gilbertson, *Environ Sci Nano*, 2017, **4**, 276-281.

5. W. Peijnenburg, A. Praetorius, J. Scott-Fordsmand, G. Cornelis, *Environ Pollut*., 2016, **218**, 1365-1369.

6. AD. Servin, JC. White, *Nano Impact*, 2016,**1**, 9-12.

7. European Commission, 2011/696/EU: Commission Recommendation of 18 October 2011 on the definition of nanomaterial, Off. J. Eur. Communities: Legis., 2011, 275, 38–40.

8. FDA. *Guidance for Industry Considering Whether an FDA-Regulated Product Involves the Application of Nanotechnology Contains Nonbinding Recommendations*.; 2014. http://www.fda.gov/RegulatoryInformation/Guidances/ucm257698.htm. Accessed January 14, 2019.

9. T. Linsinger, G. Roebben, D. Gilliland. *Requirements on Measurements for the Implementation of the European Commission Definition of the Term "Nanomaterial."*; 2012.

10. X. Chen, H.J. Schluesener, *Toxicol. Lett*., 2008, **176**, 1–12

11. B. Calderón-Jiménez, ME. Johnson, AR. Montoro Bustos, KE. Murphy, MR. Winchester, JR. Vega Baudrit, *Front Chem*., 2017, **5**, 6.

12. SA. Armitage, MA. White, HK. Wilson, *Ann. occup. Hyg.*, 1996, **40**, 331-338.

13. TT. Hoang Thi, EH. Pilkington, DH Nguyen, JS Lee, KD Park, NP. Truong, *Polymers (Basel)*, 2020, **12**, 298.

14. S. Kaga, NP. Truong, L. Esser, D. Senyschyn, A. Sanyal, R. Sanyal, JF. Quinn, TP. Davis, LM. Kaminskas, MR. Whittaker, *Biomacromolecules*, 2017, **18**, 3963–3970.

15. H. Bouwmeester, J. Poortman, RJ. Peters, E. Wijma, S. Makama, K. Puspitaninganindita, HJ. Marvin, AA. Peijnenburg, PJ. Hendriksen, *ACS Nano*, 2011, **5**, 4091–4103.

16. N. Durán, M. Durán, M. B. de Jesus, A. B. Seabra, W. J. Fávaro and G. Nakazato, *Nanomedicine*, 2016, **12**, 789–799.

17. Z. Gajdosechova, Z. Mester, *Anal Bioanal Chem.*, 2019, **411**, 4277–4292.

18. K. Loeschner, MSJ. Brabrand, JJ. Sloth, EH. Larsen, *Anal Bioanal Chem.*, 2013, **406**, 3845–3851.

19. J. Jiménez-Lamana, F. Laborda, E. Bolea, I. Abad-Álvaro, JR. Castillo, J. Bianga, H. Man, K. Bierla, S. Mounicou, L. Ouerdane, S. Gaillet, JM, Rouanet, J. Szpunar, *Metallomics*, 2014, **6**, 2242–2249.

20. J. Vidmar, T. Buerki-Thurnherr, K. Loeschner, *J Anal At Spectrom*., 2018, **33**, 752–761.

21. EP. Gray, JG. Coleman, AJ. Bednar, AJ. Kennedy, JF. Ranville, CP. Higgins, *Environ Sci Technol*., 2013, **47**, 14315-14323.

22. Z. Gajdosechova, MM. Lawan, DS. Urgast, A. Raab, KG. Scheckel, E. Lombi, PM. Kopittke, K. Loeschner, EH. Larsen, G. Woods, A. Brownlow, FL. Read, J. Feldmann, EM. Krupp, *Sci Rep*., 2016, **6**, 34361.

23. S. Makama, R. Peters, A. Undas, NW. van den Brink, *Environ Chem.*, 2015, **12**, 643.

24. F. Laborda, E. Bolea, G. Cepriá, MT. Gómez, MS. Jiménez, J. Pérez-Arantegui, JR. Castillo, *Anal. Chim. Acta*, 2016, **904**, 10–32.

25. C. Contado, *Front Chem*., 2015, **3**, 48.

26. C. Degueldre, PY. Favarger, *Colloids Surfaces A Physicochem. Eng. Asp.*, 2003, **217**, 137–142.

27. F. Laborda, E. Bolea, J. Jiménez-Lamana, *Anal Chem*., 2014, **86**, 2270-2278.

28. AR. Montoro Bustos, MR. Winchester, *Anal. Bioanal.Chem.*, 2016, **408**, 5051–5052.

29. I. Abad-Alvaro, E. Peña-Vázquez, E. Bolea, P. Bermejo-Barrera, JR. Castillo, F. Laborda, *Anal Bioanal Chem*., 2016, **408**, 5089-5097.

30. MD. Montaño, HR. Badiei, S. Bazargan, JF. Ranville, *Environ Sci Nano*., 2014, **1**, 338.

31. A. Hineman, C. Stephan, *J Anal At Spectrom*. 2014, **29**, 1252–1257.

32. DM. Schwertfeger, JR. Velicogna, A H. Jesmer, RP. Scroggins, JI. Princz, *Anal Chem*., 2016, **88**, 9908−9914.

33. HE. Pace, NJ. Rogers, C. Jarolimek, VA. Coleman, CP. Higgins, JF. Ranville, *Anal Chem*., 2011, **83**, 9361-9369.

34. MD. Montaño, JW. Olesik, AG. Barber, K. Challis, JF. Ranville, *Anal Bioanal Chem*., 2016, **408**, 5053-5074.

35. B. Meermann, V.Nischwitz, *J. Anal. At. Spectrom*., 2018, **33**, 1432.

36. M. Witzler, F. Küllmer, K. Günther, *Analytical Letters*, 2018, **51**, 587-599,

37. AR. Montoro Bustos, KP. Purushotham, A. Possolo, N. Farkas, AE. Vladar, KE. Murphy, MR. Winchester, *Anal Chem*., 2018, **90**, 14376-14386.

38. J. Liu, KE. Murphy, MR. Winchester, VA. Hackley, *Anal Bioanal Chem*., 2017, **409**, 6027-6039.

39. L. Hendriks, B. Ramkorun-Schmidt, A. Gundlach-Graham, J. Koch, RN. Grass, N. Jakubowski, D. Günther, *J Anal At Spectrom*., 2019, **34**, 716-728.

40. C. Agatemor, D. Beauchemin, *Anal Chim Acta*., 2011, **706**, 66-83.

41. P. Kościelniak, M. Wieczorek, *Anal Chim Acta*., 2016, **944**, 14-28.

42. S. Cuello-Nunez, I. Abad-Alvaro, D. Bartczak, ME. del Castillo Busto, DA. Ramsay, F. Pellegrino, H. Goenaga-Infante, *J. Anal. At. Spectrom*., 2020, **35**, 1832.

43. J. Nóbrega, MC. Santos, R. de Sousa, S. Cadore, RM. Barnes, M. Tatro, *Spectrochim. Acta, Part B*, 2006, **61**, 465–495.

44. JF. Gomes, AC. Garcia, EB. Ferreira, C. Pires, VL. Oliveira, G. Tremiliosi-Filho, LH. S. Gasparotto, *Phys. Chem. Chem. Phys*., 2015, **17**, 21683–21693.

45. M. Loula, A. Kaňa, O. Mestek, *Talanta*, 2019, **202**, 565–571.

46. F. Laborda, AC. Gimenez-Ingalaturre, E. Bolea, JR. Castillo, *Spectrochim. Acta, Part B*, 2019, **159**, 105654.

View Article Online
DOI: 10.1039/D1JA00068C

Table of contents:

14. **Table 6** Equivalent particle diameter values (average ± standard deviation, n = 9) of 40 nm PEG AgNP in the investigated media.
15. **Table 7** Number concentration and size of 40 nm PEG AgNP suspensions spiked into blood and digested with TMAH. Mean ± standard deviation (n=8-9). Recovery values are compared to the original suspension used for spiking and characterised by DMF.
16. **Table 8** Number concentration and size of 40 nm PEG AgNP suspensions in blood following 8 days storage of digests. Mean ± standard deviation (n=8-9). Recovery values are compared to the original NP suspension used for spiking. This suspension was characterised by DMF.

View Article Online
DOI: 10.1039/D1JA00068C

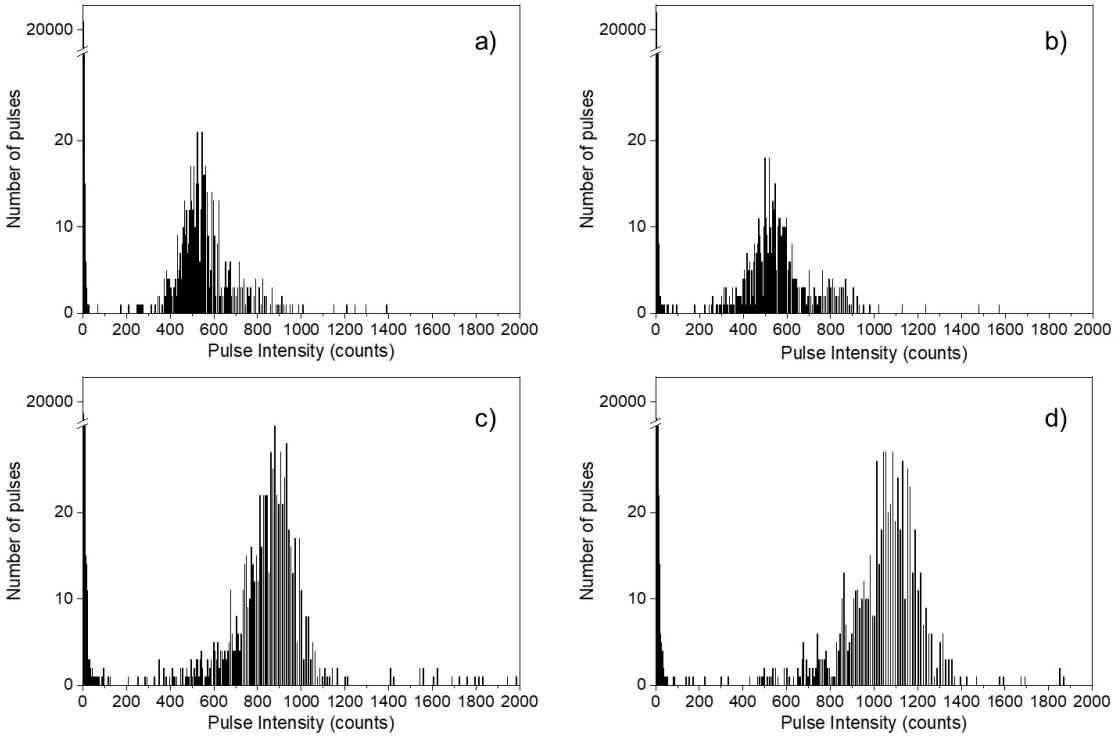

Fig. 1 Signal distribution histograms corresponding to 75 nm AgNP suspensions of 2.5 x 10^7 kg^{-1} in a) ultrapure water, b) 0.1% Triton X-100, c) 1% TMAH/0.1% Triton X-100, d) 2.5% TMAH/0.1% Triton X-100. Dwell time: 100 µs.

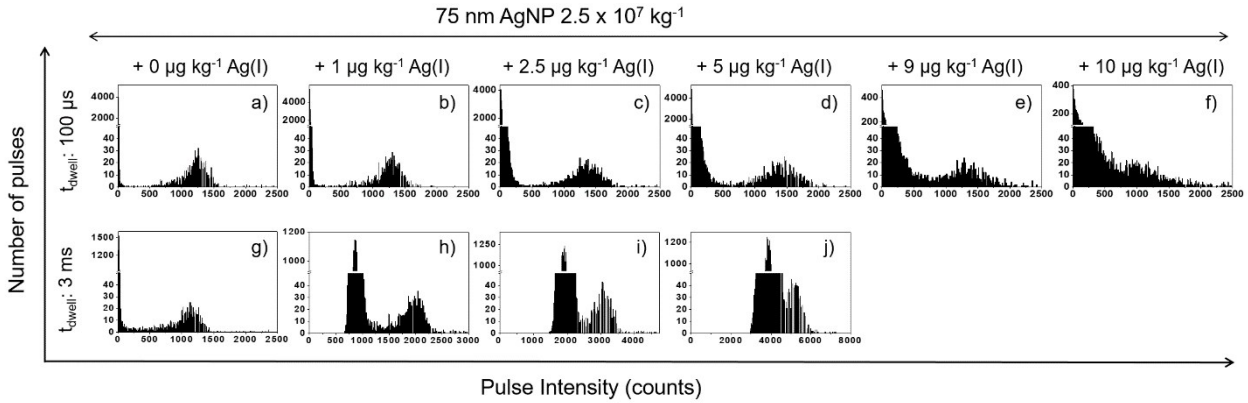

Fig. 2 Signal distribution histograms corresponding to 75 nm AgNP suspension of 2.5 x 10^7 kg^{-1} in a,g) 2.5% TMAH/0.1% Triton X-100, b,h) with 1 µg kg^{-1} Ag(I), c,i) with 2.5 µg kg^{-1} Ag(I), d,j) with 5 µg kg^{-1} Ag(I), e) with 9 µg kg^{-1} Ag(I), f) with 10 µg kg^{-1} Ag(I).

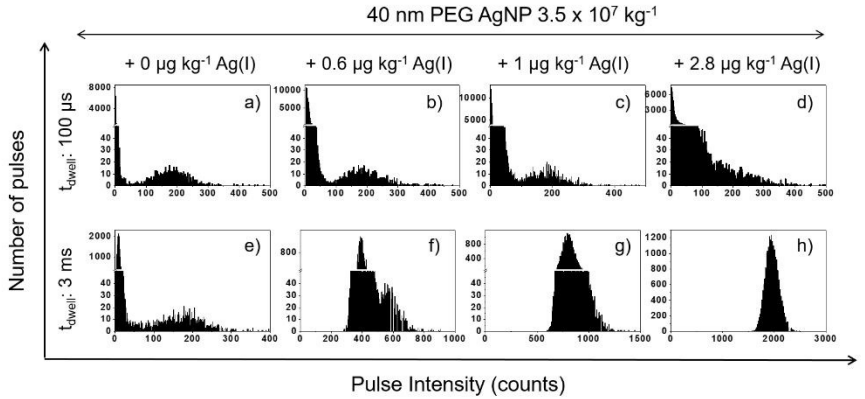

Fig. 3 Signal distribution histograms corresponding to 40 nm PEG AgNP suspension of 3.5 x 10^7 kg^{-1} in a,e) 2.5% TMAH/0.1% Triton X-100, b,f) with 0.6 µg kg^{-1} Ag(I), c,g) with 1 µg kg^{-1} Ag(I), d,h) with 2.8 µg kg^{-1} Ag(I).

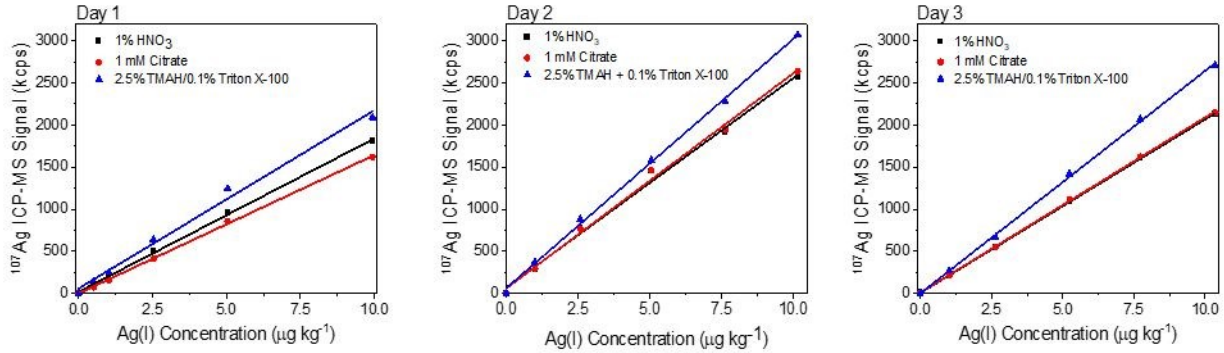

Fig. 4: Calibration curves of Ag(I) in the three different tested media. The values of sensitivity (kcps kg µg^{-1}) and R^2 (in this order) were: **Day 1:** 1% HNO_3 182 kcps kg µg^{-1} and 0.993; 1 mM trisodium citrate: 164 kcps kg µg^{-1} and 0.999; 2.5% TMAH/0.1% Triton X-100: 212 kcps kg µg^{-1} and 0.998. **Day 2:** 1% HNO_3 249 kcps kg µg^{-1}and 0.992; 1 mM trisodium citrate: 256 kcps kg µg^{-1}and 0.995; 2.5% TMAH/0.1% Triton X-100: 296 kcps kg µg^{-1} and 0.990. **Day 3:** 1% HNO_3 208 kcps kg µg^{-1}and 0.999; 1 mM trisodium citrate: 206 kcps kg µg^{-1}and 0.999; 2.5% TMAH/0.1% Triton X-100: 264 kcps kg µg^{-1}and 0.999.

View Article Online
DOI: 10.1039/D1JA00068C

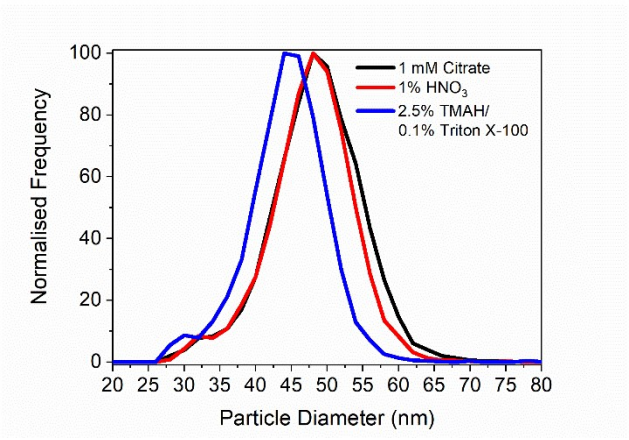

Fig. 5 Particle size distribution of 40 nm PEG AgNP in each tested matrix.

View Article Online
DOI: 10.1039/D1JA00068C

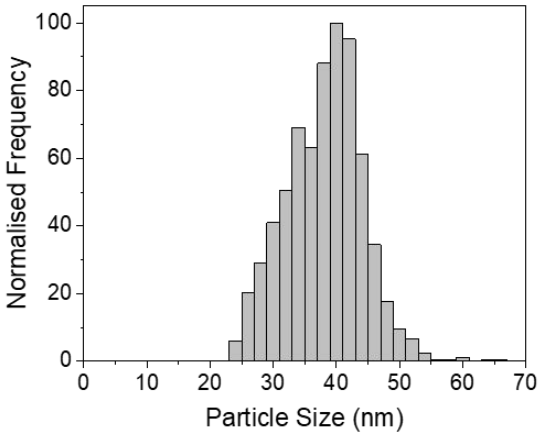

Fig. 6 Representative size distribution histogram of blood spiked with 10 µg kg^{-1} of 40 nm PEG AgNP and digested with TMAH.

View Article Online
DOI: 10.1039/D1JA00068C

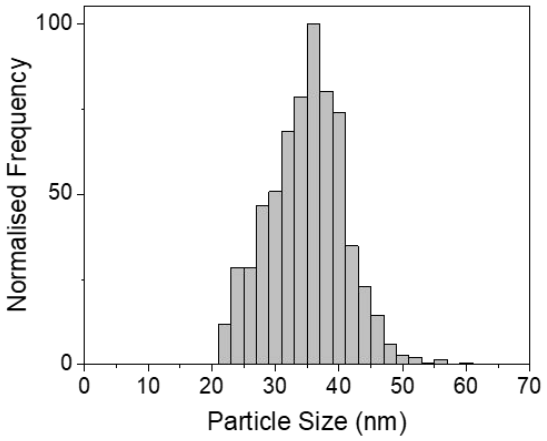

Fig. 7 Representative size distribution histogram of blood digests following 8 days storage.

View Article Online
DOI: 10.1039/D1JA00068C

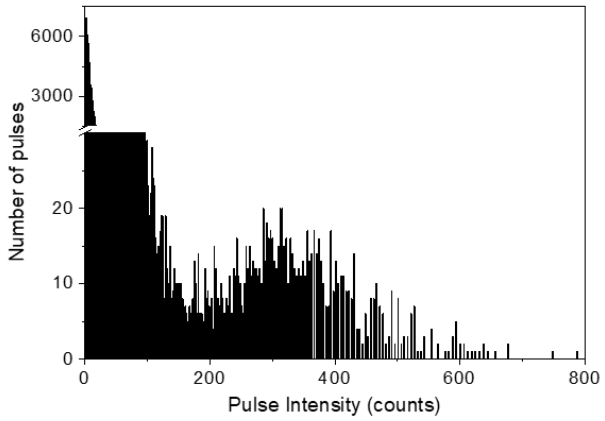

Fig. 8 Signal distribution histogram corresponding to a digested rat blood sample spiked with 4.5 x 10^7 NP kg^{-1} 40 nm PEG AgNP and 1.5 µg kg^{-1} Ag (I).

View Article Online
DOI: 10.1039/D1JA00068C

Table 1 Instrumental operating and data acquisition parameters for single-particle ICP-MS.

Instrumental parameters	
RF power	1550 W
Argon gas flow rate	
Plasma	15 L min^{-1}
Auxiliary	0.90 L min^{-1}
Nebuliser	1.10 L min^{-1}
Sample uptake rate	0.35 mL min^{-1}
Data acquisition parameters	
Dwell time	3 ms and 100 µs
Readings per replicate	20000 and 600000
Total acquisition time	60 s
Isotopes monitored	^{107}Ag

Table 2 Number of events observed for NIST RM 8017 AgNP (75 nm) in the investigated media. Mean ± standard deviation (n=5).

Medium	Number of events
Ultrapure water	586 ± 28
0.1% Triton X-100	567 ± 20
1% TMAH/0.1% Triton X-100	858 ± 21
2.5% TMAH/0.1% Triton X-100	859 ± 18

Table 3 Size limit of detection obtained for AgNP with different concentrations of Ag(I) in a matrix of 2.5% TMAH/0.1% Triton X-100.

Ag (I) concentration, μg kg^{-1}	Ratio Ag(I)/AgNP	LOD_{size}, nm	
		t_{dwell}:100 μs	t_{dwell}: 3 ms
2.5% TMAH/ 0.1% Triton	-	11	19
0.6	53	19	36
1.2	106	22	40
2.8	264	25	47
5.5	526	28	51

View Article Online
DOI: 10.1039/D1JA00068C

Table 4 Number concentration of NIST RM 75 nm AgNP suspensions in the presence of different concentrations of Ag(I). Mean ± standard deviation (n=3).

Ag(I), µg kg^{-1}	Ratio Ag(I)/AgNP	Number Concentration, kg^{-1}			
		Measured		% Recovery	
		t_{dwell}: 100 µs	t_{dwell}:3 ms	t_{dwell}:100 µs	t_{dwell}: 3 ms
0	-	(2.38 ± 0.05) x 10^7	(2.35 ± 0.07) x 10^7	99 ± 2	100 ± 3
1	19	(2.28 ± 0.07) x 10^7	(2.49 ± 0.04) x 10^7	101 ± 3	110 ± 2
2.5	48	(2.37 ± 0.09) x 10^7	(2.61 ± 0.03) x 10^7	104 ± 4	114 ± 1
5	96	(2.38 ± 0.12) x 10^7	(4.94 ± 0.10) x 10^7	103 ± 5	nc
9	175	(2.39 ± 0.10) x 10^7	nc	107 ± 4	nc
10	194	nc	nc	nc	nc

Nc: not calculated due to poor resolution between NP and background/Ag(I) distributions.

Table 5 Number concentration of 40 nm AgNP suspensions in the presence of different concentrations of Ag(I). Mean ± standard deviation (n=3).

Ag(I), µg kg^{-1}	Ratio Ag(I)/AgNP	Number Concentration, kg^{-1}			
		Measured		% Recovery	
		t_{dwell}: 100 µs	t_{dwell}:3 ms	t_{dwell}:100 µs	t_{dwell}: 3 ms
0	-	(2.73 ± 0.05) x 10^7	(2.62 ± 0.17) x 10^7	76 ± 2	73 ± 5
0.6	53	(3.11 ± 0.31) x 10^7	(2.33 ± 0.17) x 10^7	88 ± 8	nc
1.2	106	(2.96 ± 0.10) x 10^7	nc	83 ± 3	nc
2.8	264	nc	nc	nc	nc

Nc: not calculated due to poor resolution between NP and background/Ag(I) distributions.

View Article Online
DOI: 10.1039/D1JA00068C

Table 6 Equivalent particle diameter values (average ± standard deviation, n = 9) of 40 nm PEG AgNP in the investigated media.

Ionic calibration medium	Most Frequent size (nm)	Average (nm)
1 mM Citrate	47.0 ± 1.4	46.7 ± 1.6
1 % HNO_3	47.1 ± 0.5	46.7 ± 0.5
2.5% TMAH/1% Triton X-100	43.6 ± 0.6	43.3 ± 0.4

View Article Online
DOI: 10.1039/D1JA00068C

Table 7 Number concentration and size of 40 nm PEG AgNP suspensions spiked into blood and digested with TMAH. Mean ± standard deviation (n=8-9). Recovery values are compared to the original suspension used for spiking and characterised by DMF.

Sample	Number Concentration, kg^{-1}	% Recovery	Most Freq. Size, nm
40 nm PEG AgNP in 2.5%TMAH/0.1% Triton (QC)	(5.42 ± 0.15) x 10^{13}	98 ± 3	41 ± 1
Blood spiked with 0.1 µg kg^{-1} AgNP	(4.78 ± 0.33) x 10^{13}	86 ± 6	36 ± 1
Blood spiked with 10 µg kg^{-1} AgNP	(5.07 ± 0.15) x 10^{13}	91 ± 3	41 ± 1

View Article Online
DOI: 10.1039/D1JA00068C

Table 8 Number concentration and size of 40 nm PEG AgNP suspensions in blood following 8 days storage of digests. Mean ± standard deviation (n=8-9). Recovery values are compared to the original NP suspension used for spiking. This suspension was characterised by DMF.

Sample	Number Concentration, kg^{-1}	% Recovery	Most Freq. Size, nm
Blood spiked with 0.1 µg kg^{-1} AgNP	(4.98 ± 0.46) x 10^{13}	88 ± 5	33 ± 1
Blood spiked with 10 µg kg^{-1} AgNP	(5.15 ± 0.29) x 10^{13}	93 ± 8	35 ± 2

View Article Online
DOI: 10.1039/D1JA00068C

Table 9 Number concentration and size of 40 nm PEG AgNP suspensions in blood following 8 days storage of spiked samples prior digestion. Mean ± standard deviation (n=8-9). Recovery values are compared to the original suspension used for spiking. This suspension was characterised by DMF.

Sample	Number Concentration, kg^{-1}	% Recovery	Most Freq. Size, nm
Blood spiked with 0.1 µg kg^{-1} AgNP	(6.67 ± 0.59) x 10^{12}	17 ± 1	29 ± 4
Blood spiked with 10 µg kg^{-1} AgNP	(9.54 ± 0.41) x 10^{12}	12 ± 1	30 ± 6